

# Aerosol Effects on the Lifetime of Shallow Cumulus

Hongli Jiang,<sup>1</sup> Huiwen Xue,<sup>1</sup> Amit Teller,<sup>2</sup> Graham Feingold,<sup>1</sup> Zev Levin<sup>2</sup>

In Press, May 2006

---

H. Jiang, H. Xue, G. Feingold, NOAA Earth System Research Laboratory, 325 Broadway, Boulder, Colorado 80305. (Hongli.Jiang@noaa.gov; Huiwen.Xue@noaa.gov; Graham.Feingold@noaa.gov)

A. Teller and Z. Levin, Department of Geophysics and Planetary Sciences, Tel Aviv University, Tel Aviv, Israel 69978. (amit@hail.tau.ac.il; zev@hail.tau.ac.il)

<sup>1</sup>NOAA Earth System Research Laboratory,  
Boulder, CO 80305.

<sup>2</sup>Department of Geophysics and Planetary  
Sciences, Tel Aviv University, Tel Aviv, Israel  
69978.

**Abstract.** We explore the effects of increases in aerosol concentration on cloud lifetime for warm convective clouds using a two-dimensional single cloud model and three-dimensional large eddy simulations (LES). The models include size-resolved treatment of drop size distributions and warm microphysical processes. It is shown using a variety of soundings representing marine trade cumulus, and continental convective clouds that contrary to expectation, an increase in aerosol concentration from very clean to very polluted does not increase cloud lifetime, even though precipitation is suppressed. Cloud lifetimes are statistically similar although individual clouds may experience decreases in lifetime of 10–40%. An evaporation-entrainment feedback that tends to dilute polluted clouds more than clean clouds is identified. It is proposed that the small changes in cloud lifetime are due to competing effects of precipitation suppression and enhanced evaporation, with the latter tending to dominate in these shallow clouds.

## 1. Introduction

Cumulus clouds have been studied extensively because of their significant role in moisture and energy transport to the free atmosphere. They are ubiquitous in the trade wind regime, or over continental regions in response to daytime surface heating. Their coverage is on average 12% over ocean, and 5% over land [e.g., *Norris*, 1998], which is high enough to affect the global radiation budget. The effects of aerosol on cloud radiative properties and precipitation have been under scrutiny for many decades. *Warner* [1968] hypothesized that the observed decrease in cloud droplet sizes associated with biomass burning aerosol was suppressing precipitation. The development of precipitation in warm cumulus has been the focus of numerous field experiments [e.g., the Small Cumulus Microphysics Study (SCMS), *Laird et al.* 2000]. Satellite remote sensing has also been brought to bear on the problem [e.g., *Kaufman et al.*, 2005]. A systematic observational study of the effect of aerosol on shallow cumulus is complicated by the fact that cumulus clouds have an inherent variability in size and depth and the separation of aerosol from dynamical effects is challenging. Here we address this problem using numerical models. The focus is on aerosol effects on cumulus lifetime, for which very few documented observations exist. The concept of “cloud lifetime” has strong connotations in the field of climate change, and is often used synonymously with the “second aerosol indirect effect” [*Albrecht*, 1989] which states that an increase in aerosol suppresses precipitation, and increases cloud liquid water path LWP, cloud fraction CF, and cloud lifetime. However, this simple chain of events has recently been challenged for warm stratocumulus clouds [*Ackerman et al.*, 2004] and shallow cumulus [*Xue and Feingold*, 2006; *Jiang and Feingold*, 2006; henceforth XF and JF, respectively]. The latter studies confirmed a reduction in precipitation with

increasing aerosol but showed both positive and negative responses of parameters such as LWP and CF. In the following we consider the effects of cloud lifetime for both large ensembles and individual small, warm cumulus clouds generated by three different models and four soundings. This provides a fairly broad sampling of atmospheric conditions, and ensures that results are not model- or sounding-specific. The results suggest that for this cloud type lifetime is only weakly affected by aerosol. Contrary to expectation, an increase in aerosol may even result in a decrease in cloud lifetime.

## 2. Description of the Models

### 2.1. Large Eddy Simulations

Two LES models are used: (i) an adaptation of the Regional Atmospheric Modeling System (RAMS) as described in JF, hereafter referred to as RAMS@NOAA. It includes a coupled radiation model, size resolved aerosol and cloud drops (section 2.3), and a land-surface model, which makes it particularly useful for continental convective cases. (ii) The University of California Los Angeles model, UCLA-LES [*Stevens et al.*, 1999]. It is similar to RAMS@NOAA but uses simplified treatment of radiation and surface forcing. It too includes size-resolved treatment of drop size distributions (XF). It is applied to simulation of marine trade cumulus clouds where surface forcing is less variable. Both models are initiated with instantaneous pseudo-random temperature perturbations in the lowest model levels. Turbulence and subsequent cloud development typically occur after  $\sim 1\text{--}2$  hours. A field of clouds develops, enabling statistical assessment of aerosol effects on clouds. Periodic boundary conditions are applied. Configuration information for all models is provided in Table 1.

## 2.2. Single Cloud Model

TAU-2D, is the Tel Aviv University two-dimensional, non-hydrostatic, slab-symmetric cloud model [Yin *et al.*, 2000] that has been widely applied to aerosol-cloud studies. Because it only simulates single clouds it provides a rather limited view of cloud response to aerosol but it is very useful for elucidating physical processes. The model does not include radiation or surface forcing but for the short simulations performed here this is unimportant. TAU-2D is initiated with a warm bubble by applying a brief, localized temperature perturbation at the surface for anywhere between 2 s and 120 s, depending on the initial profile (Table 1).

## 2.3. Bin Microphysics

All the models employ a bin representation of the drop size distribution and associated growth processes [Tzivion *et al.*, 1987] which solves for two moments (mass and number) in each of 33 size bins. The processes of activation, condensation, collision-coalescence, breakup, and sedimentation are represented. Aerosol particles are assumed to be lognormally distributed and composed of an inorganic salt. Size distribution differences between models are negligible compared to the contrast between clean and polluted conditions.

## 3. Input Soundings

Four different soundings have been chosen, each generating clouds of different sizes, depths and precipitation (Table 1): (i) The Barbados Oceanographic and Meteorology Experiment (BOMEX) is a well-studied trade cumulus case [e.g., Siebesma *et al.*, 2003]. The sounding develops shallow cumulus clouds with depths ranging from a few 100 m to 1 km. CFs are  $\sim 10 - 15\%$ . At low aerosol concentrations ( $N_a \sim 25 \text{ cm}^{-3}$ ) clouds produce

small amounts of drizzle (cloud-averaged rainrate  $\sim 0.1 \text{ mm d}^{-1}$ ; (ii) A continental convective case from the Smoke, Aerosols, Clouds, Rainfall, and Climate (SMOCC) experiment as simulated in JF. This surface-forced case generates somewhat deeper clouds ranging from a few 100 m to 3 km and CF of  $\sim 20\%$ . Clouds with small aerosol concentrations ( $N_a \sim 100 \text{ cm}^{-3}$ ) produce local precipitation rates of up to  $100 \text{ mm d}^{-1}$ ; (iii) A Mediterranean sounding (MED) adapted from measurements in the Central Mediterranean Sea develops shallow cumulus clouds with depths and horizontal dimensions of about 500 m ; (iv) A sounding adapted from *Kogan* [1991] which produces convective clouds with a depth of about 2000 m, and horizontal dimensions of about 1500 m, i.e., significantly larger than clouds in the other soundings. The mean subcloud potential temperature gradient  $\frac{d\theta}{dz}$  (Table 1) indicates that the Kogan sounding is the most unstable, SMOCC is the most stable, and MED and BOMEX lie inbetween. The high subcloud relative humidity RH in Kogan also contributes to deeper and larger clouds.

#### 4. Methodology

In all cases models simulate a range of aerosol conditions from clean to polluted (Table 1). For the LES, we track individual clouds and calculate their sizes and lifetimes. Analysis of aerosol effects on cloud sizes has been performed by XF and JF and so we focus on effects on lifetime. In order to be defined as a cloud, columns must have  $\text{LWP} > 20 \text{ gm}^{-2}$ . Model fields are recorded at one-minute intervals to enable distinct identification of the clouds during post analysis. Cloud sizes and lifetimes are recorded over 4-hour periods. For the single-cloud TAU-2D simulations, calculation of lifetime is considered from the cloud’s incipient stage through to its decay using the same  $20 \text{ g m}^{-2}$  threshold.

## 5. Results

Figure 1 presents cloud lifetime as a function of  $N_a$  for all cases. For LES simulations, results derive from independent simulations differing only in  $N_a$ . Averages and standard deviations are calculated over  $\sim 4$  h for 100 (SMOCC) – 200 (BOMEX) clouds having lifetimes between 10 min and 40 min. Results are insensitive to the range of lifetimes chosen. Note that none of the LES results shows statistically significant changes in lifetime with increasing  $N_a$ . The variability in lifetime at any given  $N_a$  is significantly greater than the aerosol effect. TAU-2D BOMEX results are consistent with LES-BOMEX although cloud lifetimes are about one standard deviation, or 50 % larger than the mean for LES-BOMEX. Differences are due to a combination of factors such as initialization, and model configuration. For TAU-2D, Kogan and MED soundings, individual cloud lifetimes show distinct decreases (10–40%).

A second method for comparing lifetimes, where two separate LES simulations (clean and polluted) are spawned from a common dynamical point at 2 h, and individual pairs of clean and polluted clouds are tagged and followed over the course of their lifetimes, is now applied to BOMEX. This approach is closer to the TAU-2D comparisons, albeit for much larger (in this case 42) samples. Figure 2 shows that in most cases, the polluted clouds have slightly shorter lifetimes than the clean ones, consistent with the small decreases in TAU-2D BOMEX. Only two clouds behave differently. In rare cases long-lived, polluted clouds may have larger lifetimes than clean clouds (not shown) due to merging of individual clouds.

## 6. Discussion

Analysis of hundreds of warm cumulus clouds generated by three different models, based on 4 different soundings, suggests the general picture of either little to no change, or a reduction in cloud lifetime with increasing aerosol concentration, despite the decrease in precipitation. We note the importance of large statistical samples in evaluating aerosol effects, as well as the need to consider systems of dynamically interacting clouds, as with LES. The dynamical variability in the sizes and lifetimes of cumulus clouds is significantly larger than the aerosol effect. Nevertheless, the clear decrease in lifetime in some of the TAU-2D cases and LES-BOMEX (Fig. 2) suggests that distinct physical processes are at work that tend to decrease cloud lifetime. This is explored further below.

### 6.1. Evaporation-entrainment feedbacks

*Wang et al.* [2003] showed that the smaller droplets associated with polluted clouds evaporate more readily and cause higher cloud-top entrainment in stratocumulus. XF argued that this enhanced evaporation counteracts the increases in LWP associated with suppressed collision-coalescence and precipitation. Furthermore they hypothesized that the enhanced evaporation is responsible for a stronger horizontal buoyancy gradient which increases the vortical circulation around the core of cumulus clouds, and increases dilution via entrainment [Zhao and Austin, 2005]. The increase in evaporation and entrainment thus constitutes a positive feedback that acts to decrease liquid water more than is possible via the enhanced evaporation alone. The equation for vorticity  $\omega$  (in the  $y$ -direction)

$$\frac{\partial \omega}{\partial t} = -\omega \left( \frac{\partial u}{\partial x} + \frac{\partial w}{\partial z} \right) - \frac{\partial B}{\partial x}, \quad (1)$$



includes two contributions; the first from divergence, and the second from the horizontal buoyancy gradient  $\partial B/\partial x$  ( $B$  = buoyancy). Figures 3abc show mean profiles of positive and negative buoyancy averaged over 4 h (BOMEX), 5 h (SMOCC), and over the lifetime of the TAU-2D Kogan run for cloudy regions, defined *ad hoc* as cloud water mixing ratio  $> 0.01 \text{ g kg}^{-1}$  to include cloud edges and negatively buoyant air. The profiles have been normalized such that cloud base corresponds to 0 and cloud top to 1, because of the wide range in cloud heights. In all cases the polluted clouds generate larger positive and negative  $B$ , such that for clouds of similar size,  $\partial B/\partial x$  is larger for polluted clouds. (The fact that polluted clouds tend to be smaller than clean clouds - as shown by XF and JF - further strengthens this argument.) Figures 3def show the differences in  $\omega$  between clean and polluted clouds for LES (BOMEX and SMOCC) and TAU-2D (Kogan). In all cases the polluted clouds have systematically stronger positive and negative  $\omega$ . The vortical circulation around the core of the cloud is thus stronger in the case of polluted clouds. They will be more effective in entraining drier environmental air into the core of the cloud and reducing cloud water.

*Bretherton and Smolarkiewicz* [1989] showed that entrainment zones are associated with the vertical  $B$  gradient  $\partial B/\partial z > 0$ , and detrainment zones with  $\partial B/\partial z < 0$ . Figures 3ghi show the mean  $\partial B/\partial z$  for the LES and TAU-2D Kogan clouds. Polluted clouds have stronger entrainment in the lower part of the cloud than clean clouds and stronger detrainment in the upper reaches of the cloud, with the locations differing from sounding to sounding. Of interest is the fact that the TAU-2D-Kogan simulation has the largest differences between clean and polluted as well as the largest difference in cloud lifetime (Figure 1). This sounding also has the largest cloud size and driest environmental sounding

aloft (Table 1). These two factors will likely influence the response of lifetime to aerosol changes.

These results reinforce the hypothesis that the addition of aerosol to small cumulus clouds results in stronger evaporation and stronger vorticity and entrainment/detrainment. The reduction in cloud depth and width associated with increases in aerosol discussed by XF and JF suggests a positive feedback: stronger evaporation enhances vorticity and entrainment, which reduces cloud size, renders the cloud more susceptible to entrainment, and tends to reduce lifetime. These processes counter the tendency for pollution to increase cloudiness and lifetime via suppression of precipitation. It is suggested that the balance of these processes will influence aerosol effects on lifetime. It is likely that this balance will vary with the degree of precipitation, sounding, and cloud size. Thus, although adding aerosol suppresses precipitation (with the exception perhaps of giant nuclei, e.g. *Yin et al*, 2000), it cannot simply be assumed that CF and cloud lifetime will increase.

## 6.2. Relationship to Observations

In the following, we consider CF because lifetime calculations are not possible from polar-orbiting satellites, and because it is often assumed that CF and lifetime are correlated. The above results are at odds with the satellite-derived measurements of *Kaufman et al.* [2005] who showed that CF increases with increasing aerosol optical depth for warm clouds over the Atlantic. XF and JF showed cloud fraction decreasing slightly with increasing  $N_a$  and suggested that the difference may be due to the disparity in cloud sizes; *Kaufman et al.* did not analyze the small clouds simulated here. The satellite remote sensing work of *Matheson et al.* [2005] over the Atlantic shows that although CF tends

to increase with increasing aerosol in marine stratiform clouds, the reverse may be true for broken clouds closer to land. Using data derived from a 4-month average over a  $1^\circ$  box and averaged to a  $5^\circ$  box they showed that in an ocean region west of Portugal and north of Spain, and characterized by more pollution and broken clouds, CF *decreases* with increasing aerosol, while LWP is  $\sim$  constant. The drop effective radius  $r_e$  is also approximately constant, probably because the high bias artefact in  $r_e$  associated with broken (and more polluted) clouds tends to counter the expected decrease in  $r_e$  with increasing aerosol at constant LWP. Thus the *Matheson et al.* results for CF off the coast of Portugal/Spain are consistent with the results presented here. Nevertheless far more measurements will be required to place our hypotheses on a sounder footing. Given the importance of cloud radiative forcing, there is an urgent need to quantify aerosol effects on CF and cloud lifetime in different cloud regimes, using models, refined remote sensing methods and surface-based radar observations.

**Acknowledgments.** We thank Bjorn Stevens for providing the UCLA-LES model. Huiwen Xue acknowledges the National Research Council for a postdoctoral fellowship. NOAA authors acknowledge support from NOAA’s Climate Goal. Z. Levin and A. Teller acknowledge the partial support of the BSF (grant 2000 308 and the Ministry of Science in Israel (grant 01-01-01464).

## References

Ackerman, A. S., M. P. Kirkpatrick, D. E. Stevens, and O. B. Toon (2004), The impact of humidity above stratiform clouds on indirect aerosol climate forcing. *Nature*, *432*, 1014-1017.

- Albrecht, B. A. (1989), Aerosols, cloud microphysics, and fractional cloudiness, *Science*, *245*, 1227–1230.
- Bretherton and Smolarkiewicz (1989), Gravity waves, compensating subsidence and detrainment around cumulus clouds. *J. Atmos. Sci.*, *46*, 740–759.
- Jiang, H., and G. Feingold (2006), The effect of aerosol on warm convective clouds: Aerosol-cloud-surface flux feedbacks in a new coupled large eddy model. *J. Geophys. Res.*, *111*, D01202, doi:10.1029/2005JD006138.
- Kaufman, Y. J., I. Koren, L. A. Remer, D. Rosenfeld, and Y. Rudich (2005), The effect of smoke, dust, and pollution aerosol on shallow cloud development over the Atlantic ocean. *Proc. Nat. Acad. Sci.*, *102*, 11207–11212.
- Kogan, Y. L. (1991), The simulation of a convective cloud in a 3-D model with explicit microphysics. Part I: model description and sensitivity experiments. *J. Atmos. Sci.*, *48*, 1160–1189.
- Laird N. F., H. T. Ochs III, R. M. Rauber, and L. J. Miller (2000), Initial precipitation formation in warm florida cumulus. *J. Atmos. Sci.*, *57*, 3740–3751.
- Matheson, M., A., J. A. Coakley, and W. R. Tahnk (2005), Aerosol and cloud property relationships for summertime stratiform clouds in the northeastern Atlantic from Advanced Very High Resolution Radiometer observations. *J. Geophys. Res.*, *110*, D24204, doi:10.1029/2005JD006165.
- Norris, J. R. (1998), Low cloud type over the ocean from surface observations. Part II: geographical and seasonal variations. *Journal of Climate*, *11*, 383–403.
- Siebesma, A. P. et al. (2003), A large eddy simulation intercomparison study of shallow cumulus convection. *J. Atmos. Sci.*, *60*, 1202–1219.

- Stevens, B., C.-H. Moeng, and P. P. Sullivan (1999), Large-eddy simulations of radiatively driven convection: sensitivities to the representation of small scales. *J. Atmos. Sci.*, *56*, 3963-3984.
- Tzivion, S., G. Feingold, and Z. Levin (1987), An efficient numerical solution to the stochastic collection equation. *J. Atmos. Sci.*, *44*, 3139-3149.
- Wang, S., Q. Wang, and G. Feingold (2003), Turbulence, condensation and liquid water transport in numerically simulated nonprecipitating stratocumulus clouds. *J. Atmos. Sci.*, *60*, 262-278.
- Warner, J. (1968), A Reduction in Rainfall Associated with Smoke from Sugar-Cane Fires—An Inadvertent Weather Modification? *J. Appl. Meteor.*, *7*, 247-251.
- Xue, H., and G. Feingold (2006), Large eddy simulations of trade-wind cumuli: Investigation of aerosol indirect effects. *J. Atmos. Sci.*, *in press*.
- Yin, Y., Z. Levin, T. G. Reisin, and S. Tzivion (2000), The effect of giant cloud condensation nuclei on the development of precipitation in convective clouds - A numerical study, *Atmos. Res.*, *53*, 91-116.
- Zhao, M. and P. H. Austin (2005), Life cycle of numerically simulated shallow cumulus clouds. Part II: Mixing dynamics. *J. Atmos. Sci.*, *62*, 1291-1310.

**Table 1.** Summary of model configurations, initializations, and soundings

		Sounding			
	BOMEX		MED	Kogan	SMOCC
$\frac{d\theta^*}{dz}$ , K km <sup>-1</sup>	0.7		1.0	-1.3	5.0
RH <sub>sub</sub> <sup>+</sup> , %	86		84	89	73
RH <sub>free</sub> <sup>&amp;</sup> , %	28		55	17	23
Model	UCLA-LES	TAU-2D	TAU-2D	TAU-2D	RAMS@NOAA
Input aerosol range, cm <sup>-3</sup>	25; 2000	100; 2125	100; 2125	100; 2125	100; 2000
Grid: $\Delta x$ , $[\Delta y]$ , $\Delta z$ , m	100, 100, 40	40, 40	100, 100	100, 100	100, 100, 50
$\Delta t$ , s	1.5	2	2	2	2
Initialization	pseudo-random $\pm 0.2$ K	warm bubble	warm bubble	warm bubble	pseudo-random $\pm 0.2$ K
Simulation time, h	6	1.5	1.5	1.5	8
Median <sup>†</sup> cloud size, m	410	450	400	1500	450

\* Subcloud potential temperature gradient

<sup>+</sup> Subcloud mean RH.

<sup>&</sup> Mean free tropospheric RH.

<sup>†</sup> Values for TAU-2D are maximum sizes.

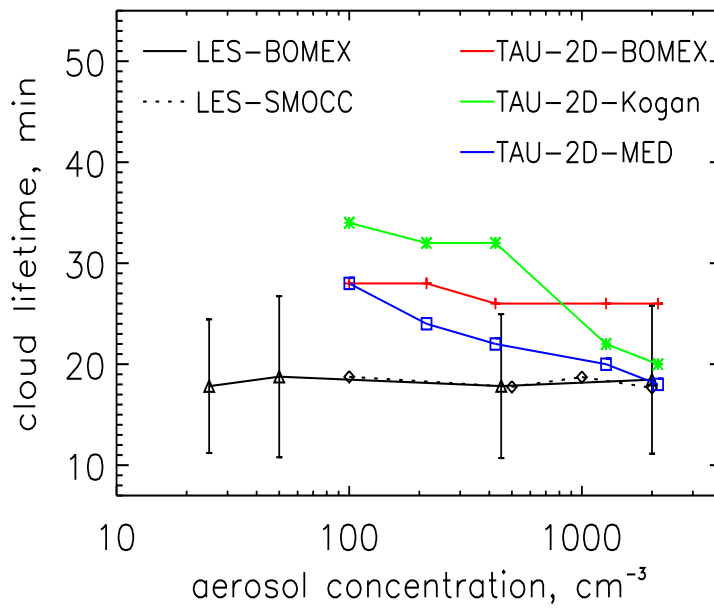


**Figure 1.** Cloud lifetime as a function of aerosol concentration  $N_a$  for all simulations. Vertical lines indicate standard deviations for LES-BOMEX; LES-SMOCC standard deviations (not shown) are of similar magnitude.

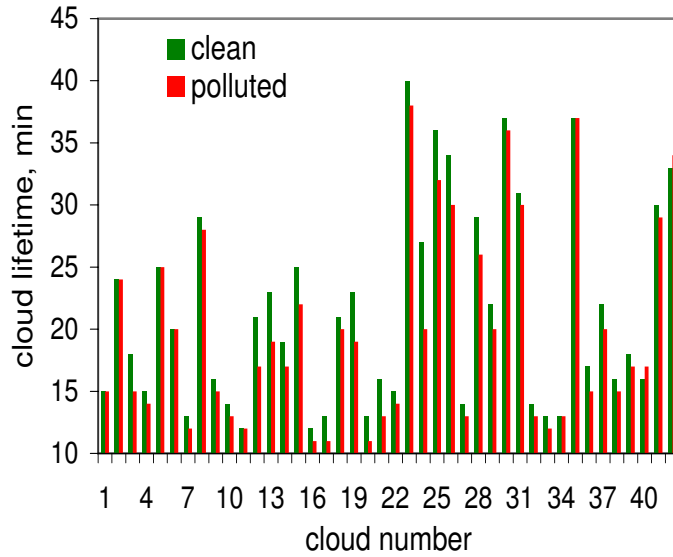


**Figure 2.** Cloud lifetime for pairs of clouds initialized from identical dynamical conditions but different  $N_a$ .

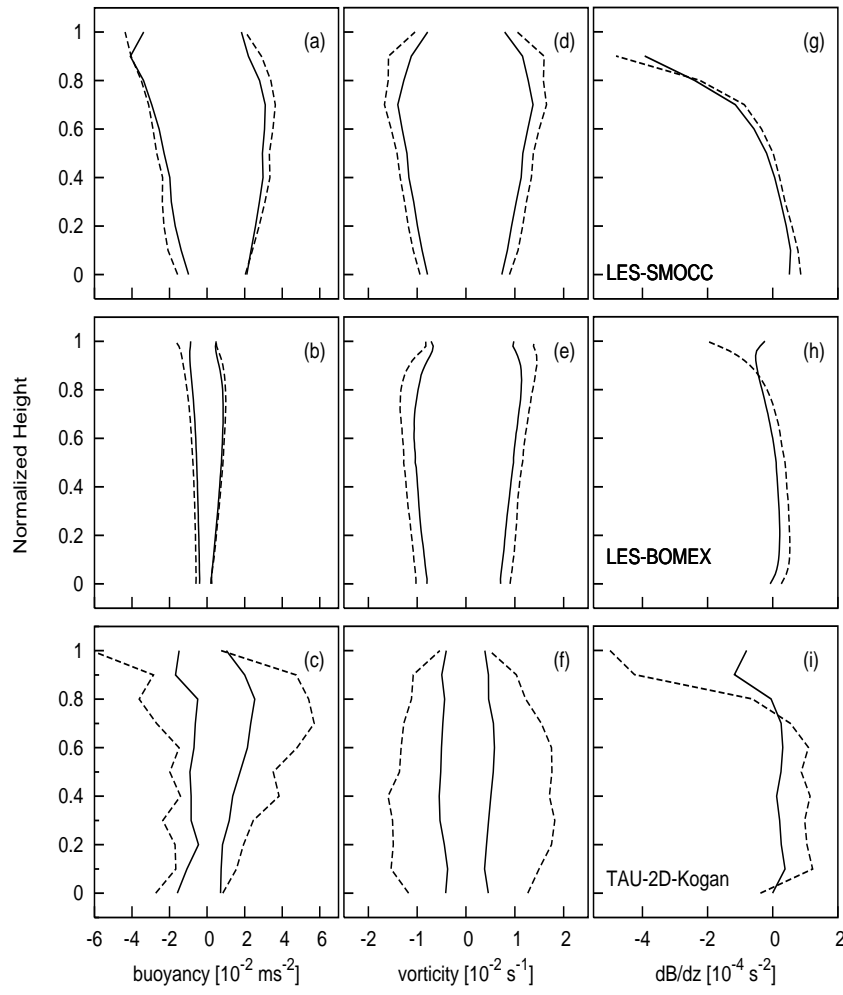


**Figure 3.** Normalized profiles of buoyancy (positive and negative) (column 1), vorticity (Eqn. 1; positive and negative) (column 2), and vertical buoyancy gradient (column 3) for LES-SMOCC, LES-BOMEX, and TAU-2D (Kogan). Dashed lines are for polluted and solid lines for clean conditions. See text for discussion.